

Effect of metal ionic radius and chelate ring alternation motif on stabilization of trivalent nickel and copper in binuclear complexes with double *cis*-oximate bridges

Olga M. Kandal, ^a Henryk Kozłowski, ^{*b} Agnieszka Dobosz, ^c Jolanta Swiatek-Kozłowska, ^c Franc Meyer ^d and Igor O. Fritsky ^{*a}

^a Department of Chemistry, National Taras Shevchenko University, 01033, Kiev, Ukraine.

E-mail: ifritsky@univ.kiev.ua; Fax: +38 044 239 33 93; Tel: +38 044 239 33 93

^b Faculty of Chemistry, University of Wrocław, F. Joliot-Curie 14, 50-383, Wrocław, Poland.

E-mail: henrykoz@wchuwr.chem.uni.wroc.pl; Fax: +48 71 3757251; Tel: +48 71 3757251

^c Department of Basic Medical Sciences, Wrocław Medical University, Kochanowskiego 14 Str., 51-601, Wrocław, Poland. E-mail: jsk@basmed.am.wroc.pl; Fax: +48 713479211;

Tel: +48 713484310

^d Institute of Inorganic Chemistry, Georg-August-University, Tammannstr. 14, D-37077,

Göttingen, Germany. E-mail: franc.meyer@chemie.uni-goettingen.de; Tel: +49 551 393012;

Fax: +49 551 393063

Received 10th December 2004, Accepted 2nd March 2005

First published as an Advance Article on the web 15th March 2005

Oxime ligands are able to form stable binuclear species with copper(II) ions in aqueous solution. They also have a strong tendency to decrease the $M^{n+/(n-1)+}$ redox potentials of the central ions. Ligands possessing the hydroxyimino groups together with other powerful σ -donor groups can be very efficient chelating agents able to facilitate the stabilisation of high oxidation states of 3d-metals. Here we report the synthesis, structural characterization and redox behaviour of mononuclear and binuclear complexes based on hydroxyiminoamide tetradentate open-chain ligands. In all mononuclear anionic complexes the central atom is situated in a square-planar surrounding of four nitrogen atoms. This pseudo-macrocyclic conformation is due to the presence of short intramolecular hydrogen bonds uniting the *cis*-oximate oxygen atoms. The square-planar surrounding of the strong σ -donors facilitates efficient stabilization of the trivalent state of copper and nickel ions. In cyclic voltammetry studies the quasi-reversible processes $M^{2+} \rightarrow M^{3+}$ can be observed. In the binuclear complexes the coordinatively saturated octahedral ion M' is bound to the two oxygen atoms of the bridging oximate groups and the four nitrogen atoms of the tetradentate ligand tren. Two metal ions (M and M') are linked by the double *cis*-oximate bridge and are incorporated in a six-membered bimetallic chelate ring. Metallamacrocyclic formation leads to certain changes in the structural parameters of the binuclear complexes as compared to those observed in the mononuclear species. Also the study of the electrochemical activity of binuclear complexes has shown important differences in their redox behaviour as compared to their mononuclear precursors.

Introduction

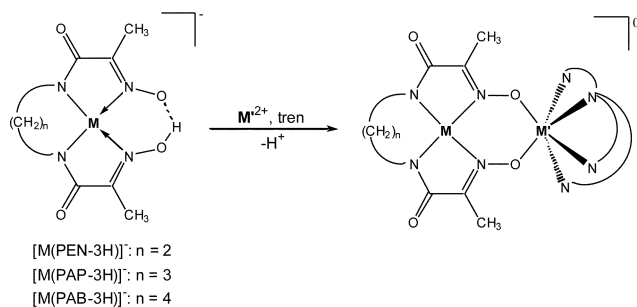
Oximes represent a very important class of ligands in coordination chemistry.¹ Recent interest in oxime ligands is mostly due to the remarkable ability of the deprotonated oximate groups to form bridges between metal ions giving rise to polynuclear complexes of different nuclearity with different types of oximate bridges.^{1a,2} The vast majority of publications on oximate complexes published during last 15 years have dealt with the synthesis and study of magnetic properties of polynuclear μ -oximate complexes. This is due to the prominent capacity of the bridging N,O-oxime function to mediate very efficiently exchange interactions between paramagnetic metal ions; in some dicopper(II) μ -oximate complexes the exchange parameters ($2J$) reach the value -1000 cm^{-1} and even higher.^{1a,2}

The strong tendency of oxime ligands to form stable binuclear species with copper(II) ions in aqueous solution due to the formation of double oximate bridges was detected for the first time in our past investigations with 2-hydroxyiminopropanoic acid, 2-cyano-2-hydroxyiminopropanoic acid, and their amide derivatives with the help of pH-potentiometry, UV-VIS and EPR spectroscopy.³

Another important feature of deprotonated oxime ligands is the strong σ -donor capacity of the nitrogen atoms resulting in a significant decrease of the $M^{n+/(n-1)+}$ redox potentials of the central ions.¹ Combining in one ligand molecule the hydroxy-

imino groups with other powerful σ -donor groups can lead to the creation of very efficient chelating agents and ligand systems facilitating stabilization of high oxidation states of 3d-metals.

Earlier we reported the synthesis, characterization and solution study of a series of copper(II) and nickel(II) mononuclear complexes based on hydroxyiminoamide tetradentate open-chain ligands and showed that these ligand systems tend to form very stable square-planar pseudo-macrocyclic complexes with the {2N(oxime),2N(amide)} donor set both in solution and in the solid state.⁴ We found that such combination of the donors in one tetradentate ligand molecule is quite efficient in stabilizing the trivalent state of nickel.⁵ Later, Krüger showed that tetradentate ligands with the same {2N(oxime),2N(amide)} donor set are efficient in the stabilization of copper(III).⁶ The mononuclear copper-(II) and -(III) complexes with these ligands have been obtained and characterized.⁶ However, up to date no bi- or polynuclear complexes with oximate bridges based on the regarded ligand systems have been reported. The effect of bridging coordination of an additional metal ion M' is expected to exhibit a certain influence both on the $M^{3+/2+}$ redox potential and the stability of the formed binuclear species containing the trivalent M (Cu^{3+} or Ni^{3+}) ions (Scheme 1). In this paper we report the synthesis, structural characterization and redox behaviour of the mononuclear $\text{PPh}_4[\text{M}(\text{L} - 3\text{H})]$ and binuclear complexes $[\text{M}(\text{L} - 4\text{H})\text{M}'(\text{tren})]$, where $M = \text{Cu}^{2+}$, Ni^{2+} ; $M' = \text{Ni}^{2+}$, Co^{3+} ; L is one of the following



Scheme 1 Formation of binuclear complexes *via* substitution of the bridging proton by metal ions.

tetradentate open-chain oxime-and-amide ligands: *N,N'*-bis(2-hydroxyiminopropanoyl)-1,2-diaminoethane (PEN), *N,N'*-bis(2-hydroxyiminopropanoyl)-1,3-diaminopropane (PAP) and *N,N'*-bis(2-hydroxyiminopropanoyl)-1,4-diaminobutane (PAB) having a different number of methylene groups (two, three or four, respectively) in the spacer between the amide functions (Scheme 1); tren is the tetradentate amine ligand tris(2-aminoethyl)amine.

Experimental

Materials and physical measurements

All chemicals were commercial products of reagent grade and used without further purification. Elemental analyses were conducted by the Microanalytical Service of the University of Wrocław. The ligands PEN, PAP and PAB were synthesized according to the reported methods.^{4a,b,7}

IR spectra (KBr pellets) were recorded on a Perkin-Elmer 180 Spectrometer in the range of 200–4000 cm^{-1} . Absorbance and diffuse-reflectance spectra were registered on a Beckman DU 650 and a Beckman UV 5240 spectrophotometers, respectively. The complex concentration was 1–3 mM.

ESI mass-spectra of the complexes (solutions in methanol) were recorded on a Finnigan MAT LCQ.

Cyclic voltammograms were obtained with an Autolab PG-STAT 12 electrochemical analyzer with GPES 4.9 software, using 2×10^{-3} M solutions in methanol at six different sweep rates ranging from 50 to 1000 mV s^{-1} . The working electrode was a Pt electrode (2-mm diameter) with an Ag/AgCl reference electrode. NBu_4PF_6 and methanol were used as the supporting electrolyte and solvent, respectively. The redox potential of the ferrocene-ferrocenium redox couple under these conditions was found to be equal to +0.410 V. The measurements were performed at 25 °C, under nitrogen.

EPR spectra were recorded at 295 and 77 K (liquid nitrogen) on a Bruker ESP 300E spectrometer at X-band frequency (9.3 GHz). Ethylene glycol–water (1 : 2 v/v) or DMSO were used as solvents for solution studies. Sample concentrations were similar to those used in spectrophotometric studies. Powdered samples were inserted in quartz sample tubes (id: 3.5 mm, od: 5 mm). The Bruker spectrometer was equipped with a Bruker NMR gaussmeter ER 035M and a Hewlett-Packard microwave frequency counter HP 5350B.

Preparation of the complexes

Li[Ni(PEN – 3H)]·4H₂O (1). This complex was synthesised according to ref. 4b.

PPh₄[Ni(PAP – 3H)]·H₂O (2), PPh₄[Ni(PAB – 3H)]·H₂O (3a) and AsPh₄[Ni(PAB – 3H)]·3.5H₂O (3b). A solution of the respective ligand (PAP 0.244 mg, 1 mmol or PAB·2H₂O 0.286 g, 1 mmol) in 10 ml of water was heated to 90 °C and added with stirring to the solution of nickel(II) nitrate hexahydrate (0.291 g, 1 mmol) in water (5 ml), then an aqueous solution of sodium hydroxide (4 ml, 1 M) was added. The obtained

mixtures were stirred at 60–80 °C for 10 min, then a solution of PPh₄Br (0.419 g, 1 mmol) or AsPh₄Br (0.463 g, 1 mmol) in 10 ml of water–methanol (10 : 1) was added. The obtained solutions were cooled, filtered and set aside for crystallization at room temperature. The resulting amber–yellow crystalline products were separated by filtration, washed with water and air-dried. The products are fairly soluble in alcohols, acetonitrile, chloroform and hot water. Yield 58% for **2** and 53% for **3a**. X-Ray analysis revealed the presence of **2** in two polymorphic crystal modifications: monoclinic (**2a**) and triclinic (**2b**).

PPh₄[Ni(PAP – 3H)]·H₂O (2). Calc. for C₃₃H₃₅N₄O₅PNi: C, 60.30; H, 5.37; N, 8.52; Ni, 8.93. Found: C, 60.50; H, 5.44; N, 8.38, Ni 9.09%. ESI-MS: *m/z* (%): 299.0 (100) [⁵⁸Ni(PAP – 3H)]⁺, 301.0 (44) [⁶⁰Ni(PAP – 3H)]⁺.

PPh₄[Ni(PAB – 3H)]·H₂O (3a). Calc. for C₃₄H₃₇N₄O₅PNi: C, 60.83; H, 5.55; N, 8.35, Ni, 8.74. Found: C, 60.58; H, 5.66; N, 8.71, Ni, 8.89%. ESI-MS: *m/z* (%): 313.0 (100) [⁵⁸Ni(PAB – 3H)]⁺, 315.0 (42) [⁶⁰Ni(PAB – 3H)]⁺.

[Li(H₂O)₄][Cu(PAP – 3H)]·2H₂O (4a) and PPh₄[Cu(PAP – 3H)]·4.5H₂O (4b). **4a** was synthesised according to.^{4a} **4b** was prepared by methathesis between **4a** and PPh₄Br in warm 10% aqueous methanolic solution. **4b** was formed as an orange crystalline material within 24 h by slow evaporation of the obtained mixture at room temperature.

PPh₄[Cu(PAP – 3H)]·4.5H₂O (4b). Calc. for C₃₃H₄₁N₄O_{8.5}PCu: C, 54.73; H, 5.71; N, 7.74; Cu, 8.77. Found: C, 54.51; H, 5.77; N, 7.91, Cu 8.99%. ESI-MS: *m/z* (%): 304.0 (100) [⁶³Cu(PAP – 3H)]⁺, 306.0 (47) [⁶⁵Cu(PAP – 3H)]⁺.

[Ni(tren)Ni(PEN – 4H)]·2H₂O (5) and [Co(tren)Ni(PEN – 4H)](ClO₄)·H₂O (6). Nickel(II) nitrate hexahydrate (0.291 g, 1 mmol) or cobalt(II) perchlorate hexahydrate (0.366 g, 1 mmol) dissolved in ethanol (10 ml) was added to a solution of tren (0.146 mg, 1 mmol) in ethanol (5 ml). A mixture of solutions of nickel(II) nitrate hexahydrate (1 ml, 1 M aqueous), PEN (1 ml, 1 M in MeOH) and aqueous NaOH (4 ml, 1 M) was prepared separately with consequent heating at 50 °C and stirring for 10 min. The two obtained solutions were then mixed, stirred for 30 min in the air on heating, then cooled, filtered and left for crystallization at room temperature. The crystals formed after 48 h were filtered off, washed with ethanol and dried in air. The complexes are soluble in water and methanol on heating. Yield 64% for **5** and 67% for **6**.

[Ni(tren)Ni(PEN – 4H)]·2H₂O (5). Calc. for C₁₄H₃₂N₈O₆-Ni₂: C, 31.98; H, 6.13; N, 21.31; Ni, 22.32. Found: C, 32.30; H, 5.94; N, 21.18; Ni, 22.49%. ESI-MS: *m/z* (%): 489.1 (2) [⁵⁸Ni₂(M)] + H⁺, 511.1 (9) [⁵⁸Ni₂(M)] + Na⁺, 1001.2 (100) [⁵⁸Ni₃⁶⁰Ni(M)₂] + Na⁺, 1491.3 (75) [⁵⁸Ni₄⁶⁰Ni₂(M)₃] + Na⁺, 1981.4 (9) [⁵⁸Ni₅⁶⁰Ni₃(M)₄] + Na⁺.

[Co(tren)Ni(PEN – 4H)](ClO₄)·H₂O (6). Calc. for C₁₄H₃₀N₈O₇ClCoNi: C, 27.68; H, 4.98; N, 18.44; Co, 9.70; Ni, 9.66. Found: C, 27.55; H, 5.06; N, 18.71; Co, 9.85; Ni, 9.60%. ESI-MS: *m/z* (%): 489.1 (100) [⁵⁹Co⁵⁸Ni(M)]⁺, 977.2 (6) [⁵⁹Co₂⁵⁸Ni₂(M)₂]²⁺ – H⁺.

[Co(tren)Cu(PAP – 4H)](NO₃)·0.25LiNO₃·6.25H₂O (7). The synthesis was carried out analogously to **6** using copper(II) nitrate instead of nickel(II) nitrate, PAP instead of PEN, and LiOH as alkali. Yield 68%.

[Co(tren)Cu(PAP – 4H)](NO₃)·0.25LiNO₃·6.25H₂O (7). Calc. for C₁₅H_{42.5}N_{9.25}O₁₄Li_{0.25}CuCo: C, 25.71; H, 6.11; N, 18.49; Co, 8.41; Cu, 9.07. Found: C, 25.70; H, 6.14; N, 18.48; Co, 8.66; Cu, 9.04%. ESI-MS: *m/z* (%): 508.1 (100) [⁵⁹Co⁶³Cu(M)]⁺, 1015.2 (5) [⁵⁹Co₂⁶³Cu₂(M)₂]²⁺ – H⁺.

X-Ray crystallography

X-Ray data were collected on a KUMA KM-4CCD diffractometer⁸ with graphite-monochromatic Mo-K α radiation ($\lambda = 0.71073 \text{ \AA}$) using the ω - 2θ technique at 293 (**5**, **6**) or 192 (**7**) K. The data collection was made using Oxford diffraction programs.^{9,10} The structures were solved by direct methods (SHELXS-97)¹¹ and refined by full-matrix least-squares on all F_o^2 (SHELXL-97)¹² anisotropically for all non-hydrogen atoms. In the structures **2a** and **3b** all the hydrogen atoms were located from difference Fourier and included into refinement (excluding the C-H hydrogen atoms of the methyl groups in **3b** which were treated using the riding model). In the structures **2b**, **5** and **6** the methylene and aromatic C-H and N-H hydrogen atoms were fixed in calculated positions, the methyl C-H hydrogen atoms were placed on calculated positions and allowed to ride on the parent atom, the O-H hydrogen atoms were located from the difference Fourier map, and in **6** were fully refined isotropically while in **5** they were not refined. In the structure **7** all the C-H and N-H hydrogen atoms were located from the difference Fourier map and their thermal and positional parameters were included in the refinement (excluding the methyl hydrogen atoms of a half-occupancy methanol molecule which were allowed to ride on the parent atom). In **7** significant disorder was found in a loose region containing solvate water and methanol molecules and a non-coordinated nitrate anion; one of the water molecules with occupancy factor of 0.75 was found to share the same space with the nitrate anions of 0.25 occupancy. Only part of the O-H hydrogen atoms of solvate water molecules in **7** were observed and located from the difference Fourier map but not included into refinement. Details of crystal data and refinement are given in Table 1.

CCDC reference numbers 263427–263432.

See <http://www.rsc.org/suppdata/dt/b4/b418598f/> for crystallographic data in CIF or other electronic format.

Results and discussion

Mononuclear anionic complexes

A speciation study of complex formation between Cu²⁺ and Ni²⁺ and PAP by potentiometric titration and a variety of spectroscopic methods revealed that in the systems with both ions the most stable species dominating over a wide range of pH are square-planar anionic complexes $[M(\text{PAP} - 3\text{H})]^-$ having a short intramolecular H-bond between the *cis*-oximate oxygen atoms.^{4a} Several compounds containing these complex anions have been isolated and characterised by X-ray analysis before,^{4a-d} and some new complexes are presented in this work.

The molecular structures of the complexes **2** and **3b** are presented in Figs. 1 and 2, respectively, the selected bond lengths are given in Table 2. In all the anionic complexes the central atoms are situated in a square-planar surrounding of four nitrogen atoms belonging to the deprotonated amide and oxime groups of the triply deprotonated residues of the ligands which adopt a pseudo-macrocyclic conformation due to the presence of short intramolecular H-bonds uniting the *cis*-oximate oxygen atoms. The most important differences in the molecular structures of the nickel complexes with the three ligands lie in the different motifs of the chelate ring alternations (5,5,5 in **1**; 5,6,5 in **2** and 5,7,5 in **3b**), and, as a consequence, in importantly different separations O(1) \cdots O(4) between the oxime oxygens involved in the intramolecular H-bonds. In the PEN-containing complex **1** this separation (2.625(2) \AA) is markedly larger than in the case of PAP- and PAB-containing complexes **2** and **3b** (2.412(3)–2.449(2) \AA). In the latter the observed values are close to those typical for the square-planar nickel(II) oximate complexes (2.43–2.48 \AA).^{4a,d,13,14} It is evident that such differences are conditioned by the presence of three fused five-membered chelate rings in **5** which makes the complex anion in **1** the most compressed and tensed and thus requires

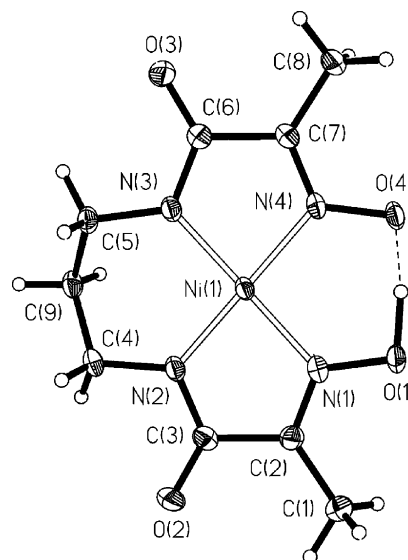


Fig. 1 Molecular structure and numbering scheme for complex **2**.

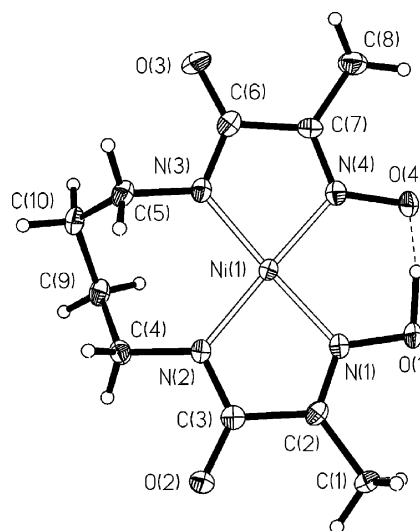


Fig. 2 Structure and numbering scheme for complex **3b**.

significant stretching of the oxygen atoms. In contrast, in **3b** the O(1) \cdots O(4) separation is somewhat shortened (2.412(3) \AA). It is evident that the difference in separations between the *cis*-oximate oxygen atoms can have a substantial impact on the reactivity of the anionic complexes in reactions of the bridging proton in substitution by metal ions of certain ionic radii.

Another consequence of tension caused by the presence of three five-membered rings in **1** are noticeably shortened Ni–N distances compared to **2b** and **3b** (Table 2), a significant decrease of the bite angle N(2)–Ni–N(3) (less than 90° , while in **2** and **3b** it is notably larger than 90°) and an increase of the opposite angle N(1)–Ni–N(4) ($102.74(7)^\circ$ in **1** vs. $96.93(7)^\circ$ and $95.51(9)^\circ$ in **2b** and **3b**, respectively). It is evident that this effect correlates with changes of the number of atoms in the internal chelate rings. In contrast, the values of the bite angles N(1)–Ni–N(2) and N(3)–Ni–N(4) in the five-membered rings in **1** are increased ($84.51(7)^\circ$ and $85.50(7)^\circ$) as compared to **2b** ($83.37(8)^\circ$ and $83.28(7)^\circ$) and **3b** ($82.69(9)^\circ$ and $82.64(10)^\circ$). However the bonding parameters of **2b** and **3b** are not significantly different. In **3b** the Ni–N distances are somewhat lengthened, especially one of the Ni–N(amide) distances (Ni–N(2) 1.909(2) \AA). This effect can be attributed to the presence of the asymmetric seven-membered chelate ring involving the Ni–N(amide) bonds in **3b**.

The structural differences in **1**, **2b** and **3b** caused by the different size of the internal chelate rings are also revealed by comparison of distortions of the corresponding coordination

Table 1 Crystal and structure refinement for complexes **2a**, **2b**, **3b**, **5**, **6** and **7**

	PPh ₃ [Ni](PAP) – 3H ₂ O (2a) ^a	PPh ₃ [Ni](PAP) – 3H ₂ O (2b) ^a	AsPh ₃ [Ni](PAB) – 3H ₂ O (3b)	[Ni(tren)Ni(PEN) – 4H ₂ O]·2H ₂ O (5)	[Co(tren)Ni(PEN) – 4H ₂ O](ClO ₄)·H ₂ O (6)	[Co(tren)Cu(PAP) – 4H ₂ O] (NO ₃)· 0.25LiNO ₃ ·6.25H ₂ O (7)
Empirical formula	C ₃₃ H ₃₅ N ₄ NiO ₃ P	C ₃₃ H ₃₅ N ₄ NiO ₃ P	C ₃₄ H ₄₂ AsN ₄ NiO _{7.50}	C ₁₄ H ₃₂ N ₈ Ni ₂ O ₆	C ₁₄ H ₃₀ N ₈ O ₉ ClCoNi	C ₁₅ H _{42.5} N _{9.25} O ₁₄ CuCoLi _{0.25}
<i>M</i>	657.33	657.33	760.35	525.90	607.55	700.79
Crystal system	Monoclinic	Triclinic	Monoclinic	Monoclinic	Triclinic	Tetragonal
Space group	<i>P</i> 2 ₁ / <i>c</i>	<i>P</i> $\bar{1}$	<i>C</i> 2/ <i>c</i>	<i>P</i> 2 ₁ / <i>n</i>	<i>P</i> $\bar{1}$	<i>I</i> 4 ₁ / <i>a</i>
<i>a</i> /Å	10.812(2)	11.539(2)	22.274(4)	7.743(2)	7.979(2)	19.8716(8)
<i>b</i> /Å	21.043(4)	12.188(2)	20.539(4)	14.627(3)	11.528(2)	19.8716(8)
<i>c</i> /Å	14.031(3)	12.527(3)	15.231(3)	19.177(4)	12.454(2)	29.6313(17)
<i>a</i> /°	90	61.69(3)	90	90	85.93(3)	90
<i>β</i> /°	109.89(3)	75.10(3)	97.18(3)	96.77(3)	81.40(3)	90
<i>γ</i> /°	90	76.22(3)	90	90	80.95(3)	90
<i>V</i> /Å ³	3001.9(10)	1484.8(5)	6913(2)	2156.8(8)	1117.2(4)	11700.8(9)
<i>Z</i>	4	2	8	4	2	16
<i>D</i> _c /g cm ⁻³	1.454	1.470	1.461	1.620	1.806	1.591
<i>μ</i> /cm ⁻¹	7.49	7.57	15.66	17.94	17.70	13.71
<i>F</i> (000)	1376	688	3160	1104	628	5856
<i>θ</i> Range for data collection/°	3.50–28.59	3.45–28.34	3.35–28.44	2.99–28.99	1.66–32.10	2.00–30.51
Reflections collected	20588	10292	23778	13666	5822	9113
Unique reflections/parameters	7014/537	6536/403	8079/571	5260/274	5822/317	8943/563
GOF	1.090	1.045	1.046	1.118	1.053	1.130
Final indices [<i>I</i> > 2σ(<i>I</i>)]	<i>R</i> 1 = 0.0355, <i>wR</i> 2 = 0.0765	<i>R</i> 1 = 0.0356, <i>wR</i> 2 = 0.0979	<i>R</i> 1 = 0.0419, <i>wR</i> 2 = 0.1262	<i>R</i> 1 = 0.0477, <i>wR</i> 2 = 0.1262	<i>R</i> 1 = 0.0282, <i>wR</i> 2 = 0.0716	<i>R</i> 1 = 0.0454, <i>wR</i> 2 = 0.1118
Final indices (all data)	<i>R</i> 1 = 0.0512, <i>wR</i> 2 = 0.0818	<i>R</i> 1 = 0.0431, <i>wR</i> 2 = 0.1019	<i>R</i> 1 = 0.0616, <i>wR</i> 2 = 0.0982	<i>R</i> 1 = 0.0513, <i>wR</i> 2 = 0.1314	<i>R</i> 1 = 0.0327, <i>wR</i> 2 = 0.0746	<i>R</i> 1 = 0.0700, <i>wR</i> 2 = 0.1268
Max., min. residual electron density/e Å ⁻³	0.367, –0.359	0.389, –0.713	0.800, –0.616	0.928, –0.869	0.960, –0.360	0.754, –0.673

^a Two polymorphic modifications.

Table 2 Selected bond lengths (Å) and valence angles (°) of the mononuclear complexes

	Li[Ni(PEN – 3H)]·4H ₂ O (1) ^a	PPh ₄ [Ni(PAP – 3H)]·H ₂ O (2b)	AsPh ₄ [Ni(PAB – 3H)]·3,5H ₂ O (3b)	[Li(H ₂ O) ₄][Cu(PAP – 3H)]·2H ₂ O (4a) ^b
M–N(1)	1.839(2)	1.8782(17)	1.879(2)	1.962(4)
M–N(2)	1.816(2)	1.8648(18)	1.909(2)	1.927(4)
M–N(3)	1.803(2)	1.8676(17)	1.878(2)	1.910(4)
M–N(4)	1.841(2)	1.8717(18)	1.881(2)	1.954(4)
O(1)–N(1)	1.372(2)	1.355(2)	1.352(3)	1.380(5)
O(4)–N(4)	1.354(2)	1.356(2)	1.363(3)	1.362(5)
O(2)–C(3)	1.255(2)	1.248(2)	1.273(3)	1.246(6)
O(3)–C(6)	1.243(2)	1.255(2)	1.248(3)	1.258(6)
N(1)–C(2)	1.283(2)	1.294(3)	1.285(3)	1.272(7)
N(4)–C(7)	1.285(3)	1.289(3)	1.283(3)	1.276(6)
O(1)···O(4)	2.625(2)	2.449(2) 2.431(2) ^c	2.412(3)	2.581(5)
O(1)–H(1)	1.061(2)	1.13(4) 1.20(4)	1.16(4)	1.087(4)
H(1)···O(4)	1.582(2)	1.33(4) 1.24(4)	1.27(4)	1.534(4)
O(1)–H(1)···O(4)	166.3(1)	172(4) 173(3)	169(3)	160.1(2)
N(1)–M–N(2)	84.51(7)	83.28(7)	82.69(9)	81.6(2)
N(1)–M–N(3)	171.73(7)	175.97(7)	173.70(9)	173.8(2)
N(1)–M–N(4)	102.74(7)	96.93(7)	95.51(9)	96.8(2)
N(2)–M–N(3)	87.25(8)	96.69(8)	99.58(9)	98.6(2)
N(2)–M–N(4)	172.74(7)	176.28(7)	175.44(9)	176.8(2)
N(3)–M–N(4)	85.50(8)	83.37(8)	82.64(10)	82.7(2)

^a Ref. 4b, numbering scheme corresponds to Fig. 3. ^b Ref. 4a, numbering scheme corresponds to Fig. 1. ^c In polymorphic modification **2a**.

spheres and the chelate ring conformations. In **1** the square-planar coordination sphere and all three chelate rings are virtually planar; realization of such conformation is necessary in order to satisfy the fused disposition of three five-membered rings. In **2b** and **3b** the equatorial planes exhibit insignificant tetrahedral distortion with deviations of the nitrogen atoms from the mean planes defined by them by 0.0630(8)–0.0845(11) Å.

Regarding the earlier published molecular structure of the anionic complex of copper with PAP, **4a**, this exhibits the expected longer M–N distances as compared to the nickel complexes, which is due to the larger ionic radius of Cu²⁺ as compared to square-planar Ni²⁺. The observed Cu–N distances in **4a** and Ni–N distances in **2b** and **3b** are normal for the complexes with N-coordinated amide and oxime groups while Ni–N bonds in **1** are shorter than the typical value due to the reasons discussed above. Note, that in **4a** a noticeable difference in Cu–N(amide) and Cu–N(oxime) distances is observed while in the Ni complexes this difference is insignificant. The O(1)···O(4) separation in **4a** (2.581(5) Å) is much larger than in the Ni complex **2b** containing the same ligand PAP (2.449(2) Å).

Above pH 9, dissociation of the bridging oximate proton starts to proceed, and according to a speciation study, at pH 9 and higher the only abundant species for both considered metal ions are [M(PAP – 4H)]^{2–}.^{4a} However, attempts to isolate the corresponding doubly charged anionic complexes with the studied ligands from strongly alkaline aqueous or alcohol solutions in all cases results in crystallization of singly charged anionic complexes containing the [M(PAP – 3H)][–] anion. This is an indication of an important stabilizing role of the short intramolecular *cis*-oximate H-bonds on formation of the crystalline phase.

An important role of the intramolecular H-bonds in additional stabilization of the coordination sphere of mononuclear *cis*-bis(oximate) complexes is also confirmed by the results of a study of complex formation in solution and by the reactivity of the corresponding compounds.^{4a,c,d,5,13} Such a feature makes it possible to carry out various chemical reactions with participation of mononuclear *cis*-bis(oximate) complexes in which the *cis*-coordination of the oximate ligands in the equatorial plane is retained. There are numerous examples of template

ring closure reactions of *cis*-oximate groups resulting in the formation of macrocyclic or open-chain complexes (in reactions with boric acid, tin(IV) compounds, etc.), i.e. reactions in which *cis*-coordination is retained.^{1b,5,13}

The bridging oxime proton can be substituted by metal ions. In this case the second metal ion appears to be coordinated to two oxime oxygen atoms forming an additional six-membered bimetallic chelate ring. This feature has often been used in the synthesis of polynuclear oximate complexes, which are extensively studied in molecular magnetism.

Synthesis and characterisation of binuclear complexes

Interaction of the anionic oximate complexes Cat[M(L – 3H)] (Cat = PPh₄ or alkaline metal ion; M = Ni²⁺, Cu²⁺) with complex cations [M'(tren)(H₂O)₂]²⁺ (M' = Ni²⁺, Co²⁺) in aqueous media in the presence of 1 equiv. of alkali results in formation of binuclear complexes where the M and M' ions find themselves linked by the double *cis*-oximate bridge (Scheme 1). Use of a tetradentate amine ligand tren for blockage of four sites in the coordination sphere of M' allows to avoid oligo- and polymerisation and limits any interaction between the anionic and cationic complexes to the exclusive formation of binuclear species. Note, that in the case of systems with M' = Co reactions are accompanied by the oxidation of the Co ion to the trivalent state, so the resulting binuclear complexes **6** and **7** are cationic while the dinickel complex **5** is neutral.

We launched numerous attempts to obtain the target binuclear complexes according to Scheme 1 with M = Ni²⁺ and Cu²⁺ and with all the three studied ligands. It should be mentioned that we succeeded to obtain only complexes involving two out of six possible oxime-containing building blocks: [Ni(PEN – 4H)]^{2–} and [Cu(PAP – 4H)]^{2–}. In the case of Ni anionic complexes with PAP and PAB, the resulting reaction mixtures produced only mononuclear starting complexes, and ESI mass-spectrometric control reactions performed under various temperature, concentration, pH and solvents mixture conditions also revealed the presence of signals corresponding to the mononuclear species only. In Cu-containing systems, we found that the mononuclear species [Cu(PEN – 4H)][–] and [Cu(PAB – 4H)][–] appear to be not

stable enough themselves with respect to competitive complex formation reactions. On standing, aqueous and methanolic solutions containing the corresponding mononuclear complexes within several hours produce insoluble neutral complexes [Cu(PAB - 2H)]·*n*H₂O and green-coloured soluble species with an alternative {2N(oxime),2O(amide)} coordination mode. On reactions with [M'(tren)(H₂O)₂]²⁺, the processes of formation of the mentioned species are accelerated, and the obtained reaction mixtures contain complex mixtures of mononuclear compounds.

Considering the reactions of substitution of the bridging oxime proton by metal ions we should take into account the distance between the oxime oxygen atoms as an important parameter which can have critical impact on the course of these reactions. Indeed, in order to allow a smooth proceeding of the proton substitution, the considered "bite distance" should fit to the accessible range of distances suitable for chelation of a metal ion with a certain ionic radius and specific tolerance to the distortion of its coordination sphere.

The expected binuclear structure of the synthesized compounds is unambiguously confirmed not only by the results of elemental analysis, but also by a variety of spectral investigations. ESI mass-spectra of the binuclear complexes exhibit signals of molecular [M]⁺ or quasi-molecular [M + Na]⁺ or [M + H]⁺ ions with characteristic isotope distribution for the species containing two atoms of the corresponding metal in one molecule of the complex. For the cationic complexes **6** and **7** the most intense peaks (100% intensity) observed in the ESI spectra correspond to the molecular ions [⁵⁹Co⁶³Cu(M)]⁺, while in the spectrum of the neutral complex **5** the major peak corresponds to its dimeric associate with a sodium ion [{⁵⁸Ni₃⁶⁰Ni(M)₂} + Na]⁺. As in the ESI-MS only charged particles can be registered, the neutral complexes as a rule are associated with the available positively charged ions (protons or cations of alkaline metals in the case when the positive registration mode is applied). It is interesting to note that in the spectrum of **5** there are quite intense signals of trimeric [{⁵⁸Ni₄⁶⁰Ni₂(M)₃} + Na]⁺ (75%) and even tetrameric [{⁵⁸Ni₅⁶⁰Ni₃(M)₄} + Na]⁺ (9%) associates of the binuclear complexes with a sodium ion. Other signals in the ESI spectra of **5**, **6** and **7** are characterized by quite low intensities (<10%).

In the diffuse-reflectance and absorption UV-VIS spectra of the binuclear complexes **5**, **6** and **7** (Table 3) asymmetric bands are observed which is due to overlap of spectral maxima characteristic for two different chromophores present in the compounds: square-planar MN₄ (M = Ni²⁺, Cu²⁺) and octahedral M'N₄O₂ (M = Ni²⁺, Co³⁺). In **5** and **6**, positions of the absorption maxima of the bands corresponding to the square-planar Ni²⁺ chromophore are close to those observed in the mononuclear complexes (398–410 nm). In **7**, the absorption maximum at 513 nm is a result of overlap of two closely situated bands caused by CuN₄ and CoN₄O₂ chromophores, thus the observed band appears to be somewhat shifted compared to the position in the spectra of **4a** and **4b** (478–479 nm). In the absorption spectra the position of maxima are not significantly changed as compared to the reflectance spectra which suggest that the metal ions M retain their coordination environment in solution.

The EPR spectrum of the solid **4b** complex is characteristic for the orthorhombic Cu²⁺ symmetry while the Cu²⁺ centrum in complex **7** is very close to tetragonal (Table 3). In solution both Cu²⁺ sites in **4b** and **7** have very similar EPR parameters characteristic for tetragonal geometry with *g*_{||} > *g*_⊥ (Table 3).

In the IR spectra of both mono- and binuclear complexes significant high frequency shifts of the ν(NO) stretching mode vibrations as compared to the position in the spectra of the free ligands is observed (Table 3). This suggests that N-coordination of the deprotonated oxime groups is retained in the binuclear complexes and is similar to their mononuclear precursors. Compared to the spectra of the mononuclear complexes, the band ν(NO) of the binuclear **5**, **6** and **7** undergoes a shift to higher frequency (Δν = 7–22 cm⁻¹) which may be caused by the change of the coordination mode from monodentate to N,O-bridging and

Table 3 IR, UV-VIS and EPR-spectroscopic characteristics of the synthesised complexes

Compound	IR frequencies/cm ⁻¹		νO-H	UV-VIS (soln.), λ _{max} /nm (ε/dm ³ mol ⁻¹ cm ⁻¹) ^d	UV-VIS (diffuse-refl.), λ _{max} /nm	EPR parameters (powder)	EPR parameters (soln.)
	νN-O oxime ^b	νC=O Amidel ^c					
Li[Ni(PEN - 3H)]·4H ₂ O (1)	1138	1596	3220	354 (5856) ^a 380sh (4484) ^a 400sh (3836)	405sh 410sh 405sh	—	—
PPh ₄ [Ni(PAP - 3H)]·H ₂ O (2)	1135	1586	3450	398sh (1350)	410sh	—	—
PPh ₄ [Ni(PAB - 3H)]·H ₂ O (3a)	1135	1596	3432	399sh (1135)	405sh	—	—
AsPh ₄ [Ni(PAB - 3H)]·3.5H ₂ O (3b)	1135	1590	3400	410sh (3550)	410sh	—	—
[Ni(tren)Ni(PEN - 4H)]·2H ₂ O (5)	1162	1590	3320	599 (12)	595 760	—	—
[Co(tren)Ni(PEN - 4H)](ClO ₄)·H ₂ O (6)	1145	1590	3360	402sh (2650) ^e 520sh (240) ^e	510 338 ^a	—	—
[Li(H ₂ O) ₄][Cu(PAP - 3H)]·2H ₂ O (4a)	1110	1601	3320	328sh (680) 479 (136)	460	—	—
PPh ₄ [Cu(PAP - 3H)]·4.5H ₂ O (4b)	1109	1590	3490	328sh (682) 478 (142)	470	—	—
[Co(tren)Cu(PAP - 4H)](NO ₃)·0.25LiNO ₃ ·6.25H ₂ O (7)	1122	1585	3410	513 (368)	518	g = 2.041 g _⊥ = 2.076 g ₃ = 2.186 g _⊥ = 2.167 g = 2.042	g = 2.163 g _⊥ = 2.044 A = 2.16 × 10 ⁻⁴ cm ⁻¹ g _⊥ = 2.046 g = 2.175

^a Charge transfer; ^b In the free ligands: PEN, 1022; PAP, 1024; PAB, 1019 cm⁻¹; ^c In the free ligands: PEN, 1624; PAP, 1621; PAB, 1628 cm⁻¹; ^d In methanol; ^e In H₂O.

also by the effect of substitution of the bridging oxime proton which results in slight shortening of the N–O distances. The absence of peaks characteristic for the stretching mode vibrations $\nu(\text{NH})$ of the secondary amide groups as well as insignificantly small frequency shifts of the absorption bands $\nu(\text{C}=\text{O})$ “Amide I” in the spectra of the synthesised complexes as compared to their positions in the spectra of the free ligands suggests preservation of N-coordination of the deprotonated amide groups.

Molecular structures of the binuclear complexes

The molecular structures of complexes **5**, **6** and **7** are presented in Figs. 3, 4 and 5, respectively. Geometrical parameters of all the structures are listed in Table 4.

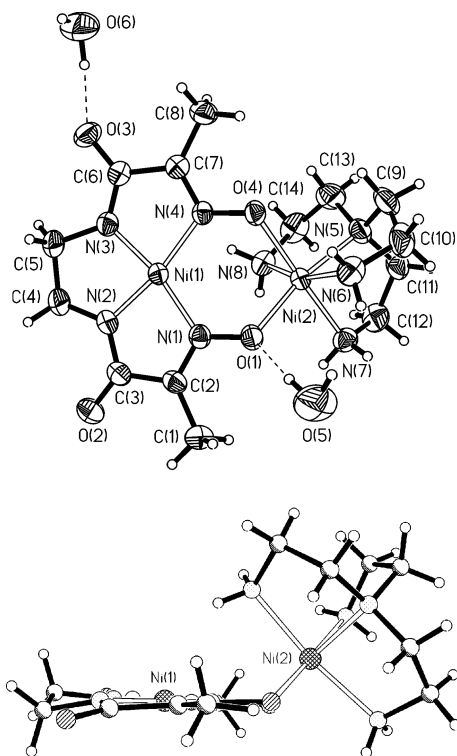


Fig. 3 Structure and numbering scheme for complex **5** (top: viewed from above with the atom-numbering scheme; bottom: side view).

Substitution of the oxime proton in the mononuclear complexes by the additional ion M' results in the closing of the coordination sphere of M $\{\text{MN}_2(\text{oxime})\text{N}_2(\text{amide})\}$ in a 13- (in the case of PEN) or 14-membered (in the case of PAP) metallamacrocyclic ring. All the binuclear complexes contain the coordinatively saturated octahedral ion M' bound to the two oxygen atoms of the bridging oximate groups, and the four nitrogen atoms of the tetradentate ligand tren. **5** is a neutral complex while **6** and **7** are anionic as they contain the trivalent Co ion. Thus, two metal ions M and M' in the binuclear complexes appear to be linked by the double *cis*-oximate bridge and incorporated in the six-membered bimetallic chelate ring.

Compared to the mononuclear precursors, the overall coordination sphere of M remains unchanged, however, macrocyclisation leads to certain changes in the structural parameters of the binuclear complexes as compared to those observed in the mononuclear complexes $[\text{M}(\text{L} - 3\text{H})]^-$. First of all, there is a significant increase in the $\text{O}(1) \cdots \text{O}(4)$ separations between the *cis*-oximate oxygen atoms on coordination of the additional metal ions M' (2.9162(17)–3.028(3) Å in the binuclear complexes vs. 2.431(2)–2.625(2) Å in the mononuclear complexes). As a consequence, a certain lengthening of the M–N distances (much more pronounced for M–N(oxime) than for M–N(amide) distances) and an increase in the values of the angles N(1)–M–N(4) (which in the binuclear complexes becomes the bite angles) is observed.

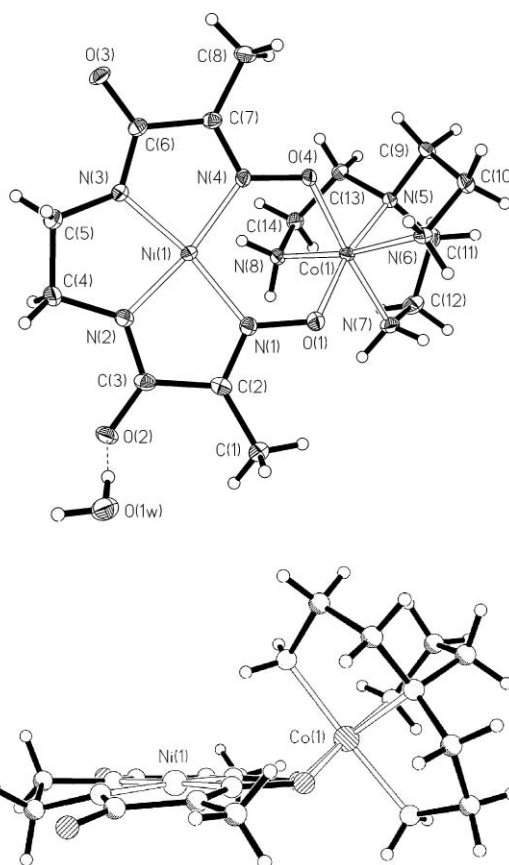


Fig. 4 Structure and numbering scheme for complex **6** (top: viewed from above with the atom-numbering scheme; bottom: side view).

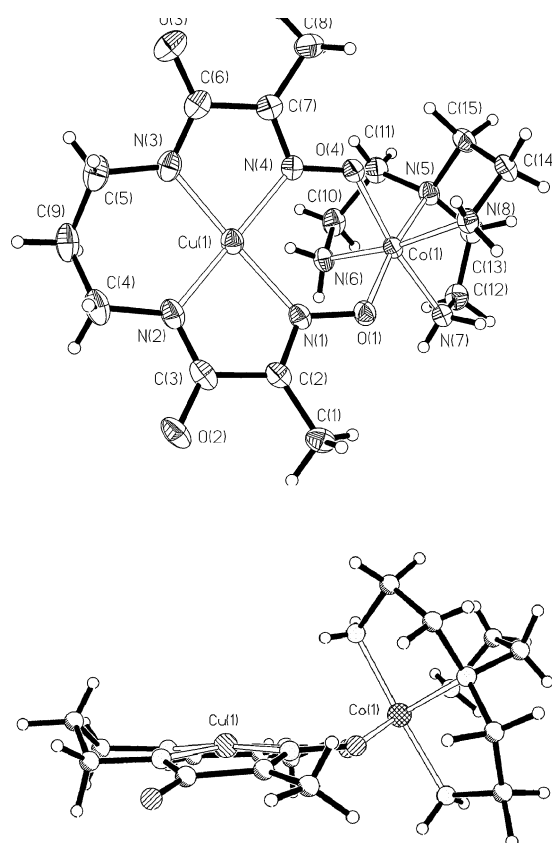


Fig. 5 Structure and numbering scheme for complex **7** (top: viewed from above with the atom-numbering scheme; bottom: side view).

Table 4 Selected bond lengths (Å) and angles (°) for **5**, **6** and **7**

	[Ni(tren)Ni(PEN – 4H)]·2H ₂ O (5)	[Co(tren)Ni(PEN – 4H)](ClO ₄)·H ₂ O (6)	[Co(tren)Cu(PAP – 4H)](NO ₃)·0.25LiNO ₃ ·6.25H ₂ O (7)
M–N(1)	1.883(2)	1.8644(15)	1.991(2)
M–N(2)	1.816(3)	1.8180(17)	1.924(2)
M–N(3)	1.829(2)	1.8201(16)	1.935(2)
M–N(4)	1.890(2)	1.8731(16)	1.972(2)
M'–O(1)	2.032(2)	1.9070(14)	1.902(2)
M'–O(4)	2.096(2)	1.9207(13)	1.898(2)
M'–N(5)	2.116(3)	1.9573(16)	1.955(2)
M'–N(6)	2.115(3)	1.9524(14)	1.952(2)
M'–N(7)	2.103(3)	1.9510(15)	1.955(2)
M'–N(8)	2.126(3)	1.9612(14)	1.946(2)
O(1)–N(1)	1.338(3)	1.345(2)	1.352(3)
O(4)–N(4)	1.329(3)	1.352(2)	1.337(3)
O(2)–C(3)	1.239(4)	1.268(2)	1.263(3)
O(3)–C(6)	1.249(3)	1.253(2)	1.259(4)
N(1)–C(2)	1.299(4)	1.314(2)	1.296(3)
N(4)–C(7)	1.309(4)	1.303(2)	1.297(4)
O(1)···O(4)	3.028(3)	2.9162(17)	2.930(3)
M···M'	3.5273(12)	3.4869(7)	3.7005(5)
N(1)–M–N(2)	83.52(11)	84.25(7)	82.75(10)
N(1)–M–N(3)	168.27(11)	169.08(7)	171.20(10)
N(1)–M–N(4)	107.00(10)	105.19(7)	98.02(9)
N(2)–M–N(3)	84.82(11)	85.42(7)	96.14(11)
N(2)–M–N(4)	169.48(11)	170.54(7)	174.49(10)
N(3)–M–N(4)	84.65(10)	85.12(7)	82.26(10)
O(1)–M'–O(4)	94.34(9)	99.26(6)	100.88(9)
O(1)–M'–N(5)	169.54(9)	169.84(6)	171.96(9)
O(1)–M'–N(6)	92.64(11)	90.29(6)	95.73(9)
O(1)–M'–N(7)	88.37(10)	83.62(6)	85.61(10)
O(1)–M'–N(8)	103.46(10)	97.95(6)	91.64(9)
O(4)–M'–N(5)	94.91(9)	89.69(6)	86.74(9)
O(4)–M'–N(6)	85.81(10)	83.77(6)	91.48(10)
O(4)–M'–N(7)	176.84(10)	175.86(6)	171.87(9)
O(4)–M'–N(8)	86.21(9)	90.17(6)	83.05(10)
N(5)–M'–N(6)	83.17(12)	85.88(6)	86.55(10)
N(5)–M'–N(7)	82.54(11)	87.20(6)	86.58(10)
N(5)–M'–N(8)	82.04(11)	86.75(6)	86.70(10)
N(6)–M'–N(7)	95.70(11)	93.27(7)	92.73(11)
N(6)–M'–N(8)	162.52(11)	170.48(6)	171.54(11)
N(7)–M'–N(8)	91.58(10)	92.38(6)	91.95(11)

Increase of the separation O(1)···O(4) in the binuclear complexes is caused by the necessity to satisfy the geometrical requirements for chelation of the M' ion of given radius, thus the values of the bite angles O(1)–M'–O(4) may be also different. For example, in the structure of the mononuclear **1** the separation O(1)···O(4) is 2.625(2) Å, while in the binuclear complexes **5** and **6** it is increased to 3.028(3) and 2.9162(17) Å, respectively. The distances Ni–N(oxime) in the coordination sphere of M are increased by 0.03–0.05 Å while the increase in Ni–N(amide) distances is only minor. In the Cu-containing complexes with PAP the separation O(1)···O(4) = 2.515(2) Å found in the mononuclear **4a** is increased to 2.930(3) Å in the binuclear complex **7**. The distances Cu–N(amide) are increased on average by 0.02–0.04 Å while Cu–N(oxime) is lengthened by 0.03–0.06 Å. The increase of the O(1)···O(4) separation influences also the angular parameters of the square-planar coordination spheres, mainly the values of the bite angles N(1)–M–N(4). In the mononuclear **1** this angle is equal to 102.74(7)° while in the binuclear complexes **5** and **6** it is increased to 107.0(1) and 105.19(7)°, respectively. In **7** the angle N(1)–Cu–N(4) (98.02(9)°) is also increased as compared to the mononuclear complex **4a** (96.8(2)°). One can show that the increase of the values of the considered angle correlates with the increase of the distance O(1)···O(4) in the polynuclear complexes (Tables 2 and 4). On the contrary, the bite angle between the coordinated amide groups N(2)–Cu–N(3) is decreased from 98.6(2)° in **4a** to 96.14(11)° in **7**.

The octahedral ions are situated in a distorted surrounding. It should be noted that the distances Co–O (1.898(2)–1.9207(13)

Å) and Co–N (1.946(2)–1.9573(16) Å) in **6** and **7** are noticeably shorter as compared to the corresponding Ni–O (2.032(2)–2.096(2) Å) and Ni–N (2.103(3)–2.126(3) Å) distances in **5**. This evidently is due to the relatively small ionic radius of Co³⁺ and also by a larger O(1)···O(4) separation in **5** (Table 4). Another consequence of the discussed effects is significant increase of the bite angle O(1)–M'–O(4) in the Co-containing complexes (99.26(6)° in **6** and 100.88(9)° in **7**) as compared to **5** (93.34(9)°). In spite of longer distances M'–O in **5** the separation Ni(1)···Ni(2) (3.527(1) Å) appears to be nearly equal to Ni(1)···Co(1) (3.4869(7) Å) in **6** and significantly shorter than Cu(1)···Co(1) in **7** (3.7006(5) Å). This could be explained in terms of two effects: noticeably shorter distances (in average by 0.1 Å) for Ni–N as compared to Cu–N in square-planar moieties and also by a different degree of folding of the bimetallic molecules along the O(1)–O(4) vector. As one can see from Figs. 3–5 (bottom), all three complexes differ noticeably by their angular conformation which can be described by the values of the dihedral angles between the planes of the corresponding bite angles MN(1)N(4) and M'O(1)O(4). These angles are 129.8(1)° in **5**, 137.62(5)° in **6** and 142.94(8)° in **7**. Such conformational differences significantly influence the values of metal–metal separations: one can observe that in the complex with the largest dihedral angle (**7**) the longest M···M' separation is realised. Slightly shorter M···M' separation in **6** compared to **5**, in spite of a larger dihedral angle along the O(1)–O(4) line is evidently conditioned by shorter metal–ligand distances in the octahedral coordination sphere of Co³⁺ in **6** as compared to Ni²⁺ in **5**.

In the structures **5** and **6** the equatorial planes of the square-planar ions M atom are nearly regular (the deviation of the atoms from the mean plane MN₄ does not exceed 0.014(1) and 0.034(1) Å, respectively, while in **7** the equatorial plane of the copper ion undergoes slight tetrahedral distortion, and the central atom is displaced by 0.121(1) Å out of the mean plane defined by the four nitrogen atoms. The central six-membered bimetallic cycles MN(1)O(1)M'O(4)N(4) in all the structures exhibit the conformation of an insignificantly distorted envelope with the M' atoms displaced from the mean planes defined by the other five atoms by 1.071(2) (in **5**), 0.850(1) (in **6**) and 0.696(2) (in **7**) Å.

Electrochemical studies

As expected, in the synthesized mononuclear anionic complexes essential thermodynamic stabilization of copper(III) and nickel(III) takes place. The square-planar surrounding of the strong σ-donors: N-coordinated deprotonated oxime and amide groups facilitates efficient stabilization of the trivalent state.

A cyclic voltammetry study of the mononuclear complexes revealed the presence of quasi-reversible processes M²⁺ → M³⁺ (M = Ni, Cu) with positions of cathodic and anodic peaks invariant with respect to different sweep rates with formal electrode potentials of +0.691–0.755 V vs. the Ag/AgCl electrode for the Ni-containing complexes **1**, **2** and **3a** and +0.485 V for the Cu-containing complex **4b** in methanol (+0.793–0.798 and +0.354 V, respectively, in acetonitrile) (Table 5). The values of the formal redox potentials M^{3+/2+} (M = Ni, Cu) suggest quite efficient thermodynamic stabilization of the trivalent state in the mononuclear complexes. Observed values for the Ni^{3+/2+} redox potentials are close to those reported for the tetraazamacrocyclic nickel(II) complexes providing a mixed N(amide)N(amine) donor environment.¹⁵ Note, that the value of E_f(Cu^{3+/2+}) observed for **4b** in acetonitrile is very close to those reported by Krüger *et al.*⁵ for the mononuclear copper complexes with open-chain ligands having the same {2N(oxime),2N(amide)} donor set but different disposition of the amide groups and having several peripheral methyl groups (0.354 mV vs. Ag/AgCl for **4b** and 0.321 mV for the complex in ref. 5). The observed formal Cu^{3+/2+} potential values are significantly lower than those found for the analogous Ni complex in the same solvents. One can see that in the Ni complex **1** having three condensed five-membered rings the +3 state is somewhat destabilized compared to **2** and **3a**, probably because the internal donor cavity is smaller than required to ideally fit the Ni³⁺ ionic radius. It should be noted that the effect of thermodynamic destabilization of square-planar mononuclear nickel(II) complexes with tetranitrogen macrocyclic ligands having three condensed five-membered chelate rings has been recognized before.¹⁶

A study of the electrochemical activity of binuclear complexes **5**, **6** and **7** in methanol revealed important differences in their redox behaviour as compared to their mononuclear precursors and also differences among the series of binuclear complexes having different M' ions. In **7**, a significant anodic shift of the redox potential compared to that seen for the Cu-containing mononuclear complex **4b** is observed (ΔE_f = +0.274 V). This effect is believed to be caused by partial electrostatic destabilization of the doubly-charged cationic species formed on oxidation of the Co³⁺-containing cationic binuclear complex. Surprisingly this effect is negligibly small in the similar Co³⁺-containing complex **6** (ΔE_f = +0.009 V vs. **1**). It is interesting to note that unlike the Co³⁺-containing complexes **6** and **7**, the dinickel binuclear complex **5** exhibits the opposite trend, and its Ni^{3+/2+} redox potential is decreased by more than 0.1 V as compared to the mononuclear complex **1** (Table 5). This effect can be understood in terms of a decrease of compression in the equatorial plane of the Ni coordination sphere on account of an increase of separation O(1)⋯O(4) between the *cis*-oxime oxygen atoms upon bridging coordination. In this way the macrocyclic cavity becomes wider and thus fits better to the size of the larger Ni³⁺ ion as compared to the mononuclear complex (Tables 2 and 4), since square-planar Ni²⁺ has a smaller ionic radius than tetragonal-bipyramidal Ni³⁺,¹⁷ having the same in-plane donor environment, which is formed on account of axial coordination of solvent molecules. On the contrary, in the Cu-containing complex **7** the stretching of the donor cavity accompanied by an increase of the Cu–N distances results in partial destabilization of the Cu(III) species formed upon electrochemical oxidation, as the Cu³⁺ ion has a smaller ionic radius than Cu²⁺ and thus fits much worse to the wider metallamacrocyclic cavity.

In this context one can explain different trends in changes of the formal redox potentials of the binuclear complexes. There are two factors affecting their values in the considered systems: (i) the effect of partial electrostatic destabilization of the cationic species formed upon oxidation which is much more pronounced in the Co³⁺-containing complexes as they produce doubly charged cationic species on oxidation; (ii) the effect of widening of the donor cavity on bridging coordination of the second metal ion M' *via cis*-oximate oxygen atoms, resulting in the lengthening of the M–N bonds. This effect has a different impact on complexes with M = Ni²⁺ and Cu²⁺: in the first case it leads to additional stabilization of the formed Ni³⁺ species as the wider cavity fits better the larger Ni³⁺ ions; in the case of Cu-containing complexes it results in additional destabilization of the Cu³⁺ species as the Cu³⁺ ions has a smaller ionic radius as compared to the Cu²⁺ ion.

Thus, in the neutral binuclear complex **5** the effect of electrostatic stabilization is insignificant and the conformational

Table 5 Redox characteristics of the synthesized mono- and binuclear complexes in methanol and acetonitrile solutions (*c* = 2 × 10⁻³ M) at sweep rate 0.100 V s⁻¹

Compound	E _a /V	E _c /V	(E _a – E _c)/V	i _a /i _c	E _f /V (vs. Ag/AgCl)
Li[Ni(PEN – 3H)]·4H ₂ O (1)	0.825	0.685	0.140	1.2	0.755
PPh ₄ [Ni(PAP – 3H)]·H ₂ O (2) ^a	0.761	0.620	0.141	1.3	0.691
	0.849 ^b	0.747 ^b	0.103 ^b	1.2 ^b	0.798 ^b
PPh ₄ [Ni(PAB – 3H)]·H ₂ O (3a) ^a	0.791	0.635	0.157	1.3	0.713
	0.864 ^b	0.722 ^b	0.142 ^b	1.3 ^b	0.793 ^b
[Ni(tren)Ni(PEN – 4H)]·2H ₂ O (5)	0.684	0.588	0.096	1.2	0.636
	0.987 ^c	0.884 ^c	0.103 ^c	1.3 ^c	0.936 ^c
[Co(tren)Ni(PEN – 4H)](ClO ₄)·H ₂ O (6) ^a	0.820	0.710	0.110	1.3	0.764
PPh ₄ [Cu(PAP – 3H)]·4.5H ₂ O (4b)	0.529	0.440	0.089	1.0	0.485
	0.393 ^b	0.315 ^b	0.078 ^b	1.0 ^b	0.354 ^b
[Co(tren)Cu(PAP – 4H)](NO ₃)·0.25LiNO ₃ ·6.25H ₂ O (7)	0.803	0.715	0.088	1.1	0.759
Ferrocene	0.449	0.371	0.078	1.0	0.410
	0.481 ^b	0.400 ^b	0.081 ^b	1.0 ^b	0.441 ^b

^a Sweep rate 0.025 V s⁻¹ in methanol, 0.500 V s⁻¹ in acetonitrile. ^b In acetonitrile. ^c Ni³⁺ → Ni⁴⁺ oxidation.

effect has evidently a larger contribution, so that the observed redox potential is decreased compared to the mononuclear complex **1**. In the case of **6**, electrostatic destabilization is much more significant, so that the contribution of electrostatic and conformational effects are approximately equal and compensate each other, and the observed redox potential does not change much compared to the mononuclear complex **1**. Finally, in **7** both electrostatic and conformational effects result in partial destabilization of the Cu trivalent state, and the observed redox potential is markedly higher than that measured for the mononuclear complex **4b**.

In the considered systems the thermodynamic stability of the binuclear complexes varies on account of a change of geometrical parameters of the coordination sphere of the redox active metal M, which is controlled by the redox-innocent metal ion M'. This may be considered as an example of allosteric regulation of the redox potential.

Consideration of structural features and electrochemical properties of the synthesized complexes may be helpful in understanding the problems which we encountered during the reactivity study. It is evident that the separation between the *cis*-oximate oxygen atoms is a very important parameter which may have a critical impact on reactivity of the mononuclear matrices and redox properties of both mono- and binuclear complexes. It is believed that this separation can be changed in a certain range of values determined mainly by the ionic radius of the central atom and the motif of the chelate ring alternation. Substitution of the bridging oxime proton by the second metal ion requires a certain stretch of the oxime oxygens, however, the extent of this stretch is sure to be limited to a certain threshold value. Thus, substitution of the oxime proton in the PEN-containing nickel(II) complex **1** is accompanied by stretching of the O(1)···O(4) separation from 2.625(2) to 2.9162(17)–3.028(3) Å, *i.e.* by 0.29–0.40 Å. In the case of the copper-containing complex **7** this stretch is equal to 0.35 Å. It is evident that in order to facilitate substitution of the bridging oxime proton by the bi- or trivalent 3d-metal ions, the mononuclear matrix should provide *cis*-interdonor distances in the range *ca.* 2.90–3.20 Å. Bridging coordination of the second metal ion to the mononuclear complexes of nickel(II) with PAP and PAB would require stretching of the O(1)···O(4) separation by at least 0.45–0.50 Å which is impossible for the ligand systems having the six- and seven-membered rings situated *trans* to the bridging oxime proton. This would probably be a satisfactory explanation of the inactivity of Ni-containing mononuclear complexes with PEN and PAP in reactions aimed at substitution of the bridging oxime proton by metal ions.

Conclusions

The mononuclear nickel(II) and copper(II) complexes with ligands having the {2N(oxime),2N(amide)} donor set indicate quite efficient thermodynamic stabilization of the +3 oxidation state of the central atoms; the differences in Ni^{3+/2+} redox potentials may be attributed to different alternation motifs of the chelate rings in the donor cavity. The mononuclear complexes appeared to be suitable precursors for obtaining the binuclear complexes *via* substitution of the bridging oxime proton by 3d-metal ions. Comparison of the structural features of the mono- and binuclear complexes revealed important differences, mostly connected with widening of the internal tetranitrogen donor cavity due to the stretch of the separation between the oxime oxygen atoms on the second ion coordination. The binuclear complexes showed noticeable shifts in the values of formal redox potentials Ni^{3+/2+} and Cu^{3+/2+} as compared to those observed in mononuclear complexes. The observed changes are explained in the terms of the electrostatic destabilization of the cationic species formed on oxidation, and in terms of effect of better or worse fit of the M³⁺ or M²⁺ ion to the size of the

metallamacrocyclic cavity. The fine tuning of redox potentials in tetragonal metal complexes may be achieved by proper control of the size of the donor cavity by use of different metal ions for its capping.

Acknowledgements

This work was performed within the COST action D21 and partially supported by a grant from the Polish State Committee for Scientific Research (grant PBZ-KBN-060/T09/2001/14) and Wrocław Medical University. I. O. F. thanks the Deutsche Akademische Austauschdienst (DAAD) for a grant within the Programme *Study Visits by Foreign Academics*.

References

- (a) *Comprehensive Coordination Chemistry II, Vol. 1, Section 1: Ligands*, ed. J. A. McCleverty and T. J. Meyer, Elsevier Science, Oxford, UK, 2004; (b) V. Yu. Kukushkin, D. Tudela and A. J. L. Pombeiro, *Coord. Chem. Rev.*, 1996, **156**, 333–362; (c) V. Yu. Kukushkin and A. J. L. Pombeiro, *Coord. Chem. Rev.*, 1999, **181**, 147–175; (d) P. Chaudhuri, *Coord. Chem. Rev.*, 2003, **243**, 143.
- (a) J.-P. Costes, F. Dahan, A. Dupuis and J.-P. Laurent, *J. Chem. Soc., Dalton Trans.*, 1998, 1307–1314; (b) E. Colacio, J. M. Domingues-Vera, A. Escuer, R. Kivekäs, M. Klinga, J.-M. Moreno and A. Romerosa, *J. Chem. Soc., Dalton Trans.*, 1997, 1685–1689; (c) B. Cervera, R. Ruiz, F. Lloret, M. Julve, J. Cano, J. Faus, C. Bois and J. Mroziński, *J. Chem. Soc., Dalton Trans.*, 1997, 395–401.
- (a) C. O. Onindo, T. Yu. Sliva, T. Kowalik-Jankowska, I. O. Fritsky, P. Buglyo, L. D. Pettit, H. Kozłowski and T. Kiss, *J. Chem. Soc., Dalton Trans.*, 1995, 3911–3915; (b) T. Yu. Sliva, A. N. Duda, T. Glowiak, I. O. Fritsky, V. M. Amirkhanov, A. A. Mokhir and H. Kozłowski, *J. Chem. Soc., Dalton Trans.*, 1997, 273–276; (c) T. Yu. Sliva, A. Dobosz, L. Jerzykiewicz, A. Karaczyn, A. M. Moreeuw, J. Świtek-Kozłowska, T. Glowiak and H. Kozłowski, *J. Chem. Soc., Dalton Trans.*, 1998, 1863–1868.
- (a) A. M. Duda, A. Karaczyn, H. Kozłowski, I. O. Fritsky, T. Glowiak, E. V. Prisyazhnaya, T. Yu. Sliva and J. Świtek-Kozłowska, *J. Chem. Soc., Dalton Trans.*, 1997, 3853–3859; (b) I. O. Fritsky, H. Kozłowski, E. V. Prisyazhnaya, Z. Rzaczyńska, A. Karaczyn, T. Yu. Sliva and T. Glowiak, *J. Chem. Soc., Dalton Trans.*, 1998, 3629–3633; (c) I. O. Fritsky, J. Świtek-Kozłowska, A. A. Kapshuk, H. Kozłowski, T. Yu. Sliva, E. Gumienna-Kontecka, E. V. Prisyazhnaya and T. S. Iskenderov, *Z. Naturforsch., Teil B*, 2000, **55**, 966–970; (d) I. O. Fritsky, J. Świtek-Kozłowska, A. Dobosz, T. Yu. Sliva and N. M. Dudarenko, *Inorg. Chim. Acta*, 2004, **346**, 111–118.
- I. O. Fritsky, H. Kozłowski, P. J. Sadler, O. P. Yefetova, J. Świtek-Kozłowska, V. A. Kalibabchuk and T. Glowiak, *Chem. Soc., Dalton Trans.*, 1998, 3269–3274.
- J. Hanss, A. Beckmann and H.-J. Krüger, *Eur. J. Inorg. Chem.*, 1999, **1**, 163–172.
- H.-P. Lau and C. D. Gutsche, *J. Am. Chem. Soc.*, 1978, **100**, 1857.
- Kuma Diffraction. Kuma KM4 software*, Kuma Diffraction, Wrocław, Poland, 1998.
- Cryp Alin Red 166*, Oxford Diffraction Wrocław.
- Cryp Alin CCD*, Oxford Diffraction Wrocław.
- G. M. Sheldrick, *SHELXS-97, Program for Crystal Structure Solution*, University of Göttingen, Germany, 1997.
- G. M. Sheldrick, *SHELXL-97, Program for Crystal Structure Refinement*, University of Göttingen, Germany, 1997.
- I. O. Fritsky, *J. Chem. Soc., Dalton Trans.*, 1999, 825.
- (a) M. S. Hussain and E. O. Schlemper, *Inorg. Chem.*, 1979, **18**, 2275–2280; (b) T. Yu. Sliva, T. Kowalik-Jankowska and V. M. Amirkhanov, *J. Inorg. Biochem.*, 1997, **65**, 287.
- (a) F. Meyer and H. Kozłowski, in *Comprehensive Coordination Chemistry II*, ed. J. A. McCleverty and T. J. Meyer, Elsevier, Oxford, UK, 2004, vol. 6, pp. 247–554; (b) E. Kimura, *J. Coord. Chem.*, 1986, **15**, 1–28; (c) R. W. Hay, R. Bembi and W. Sommerville, *Inorg. Chim. Acta.*, 1982, **59**, 147–153.
- (a) S. P. Gavrish and Ya. D. Lampeka, *J. Coord. Chem.*, 1996, **38**, 295–303; (b) S. P. Gavrish and Ya. D. Lampeka, *J. Coord. Chem.*, 1991, **24**, 351–362.
- (a) R. D. Shanon and C. T. Prewitt, *Acta. Crystallogr., Sect. B.*, 1969, **25**, 925; (b) R. D. Shanon and C. T. Prewitt, *Acta. Crystallogr., Sect. A*, 1976, **32**, 751; (c) J. E. Huheey, E. A. Keiter and R. L. Keiter, *Inorganic Chemistry: Principles of Structure and Reactivity*, Addison-Wesley Publishing Co., New York, 4th edn., 1997.